BEAM LOSS AND COLLIMATION IN THE ESS LINAC

R. Miyamoto*, B. Cheymol, H. Danared, M. Eshraqi, A. Ponton, J. Stovall, L. Tchelidze
ESS, Lund, Sweden
I. Bustinduy, ESS-Bilbao, Bilbao, Spain
H.D. Thomsen, A.I.S. Holm, S.P. Møller, ISA, Aarhus, Denmark

Abstract

The European Spallation Source (ESS), to be built in Lund, Sweden, is a spallation neutron source based on a 5 MW proton linac. A high power proton linac has a tight tolerance on beam losses to avoid activation of its components and it is ideal to study patterns of the beam loss and prepare beam loss mitigation schemes at the design stage. This paper presents simulations of the beam loss in the ESS linac as well as beam loss mitigation schemes using collimators in beam transport sections.

INTRODUCTION

The European Spallation Source (ESS) will be a spallation neutron source based on a 5 MW proton linac, planned to be constructed in Lund, Sweden [1]. Design of the linac has been updated under the ESS Accelerator Design Update Project, a collaboration between universities and institutions in five European countries with additional contributions and supports from accelerator laboratories inside and outside of Europe. The project is near the completion and the updated design will be presented in the ESS Technical Design Report, published at the end of 2012 together with a cost report, time schedule and other documents needed for the final approval of the construction of ESS.

Figure 1 shows the schematic layout of the ESS linac [2] which consists of room temperature accelerating structures, an iron source (IS), radio frequency quadrupole (RFQ), and drift tube linac (DTL), and a superconducting linac (SCL), including spoke, medium β, and high β elliptical cavities, together with low, medium and high energy beam transport (LEBT, MEBT and HEBT) sections.

One of the toughest challenges in design and operation of a high power proton linac is to minimize beam losses. *Fast losses* (infrequent, short term, and high power losses mostly from fault scenarios) from a 5 MW proton beam could damage the linac components quite fast [3], and so a machine protection system which detects anomalies in the linac and stops the beam operation is a critical system but is not in scope of this paper. *Slow losses* (continuous and low power losses) which do not damage the components may still produce radioactive nuclei inside the components and prevent hands-on maintenance after a reasonable cooling time. Minimizing the slow losses requires a lot of efforts in various aspects and on-going efforts include 1) identifying the loss limit based on the activation level of components, 2) understanding the correlation between the losses and the beam and lattice conditions, 3) preparing collimators to remove halo particles, and 4) preparing diagnostics devices and strategies. This paper presents status of the efforts 1), 2), and 3).
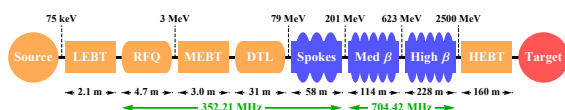
BEAM LOSS LIMIT IN RFQ AND DTL

A study is conducted to estimate the beam loss limit in the RFQ and DTL which allows the hands-on maintenance by radiation workers after a reasonable cool down time (four hours are assumed) [4] and to re-evaluate the often quoted 1 W/m loss criteria. Two documents [5, 6] specify ionizing radiation does limits for radiation works at ESS but, in the following study, a more restricted limit of CERN for supervised temporary workplace, 15 μSv/hr measured 40 cm from an accelerating structure, is used.

The relation between the beam loss and radiation does on the outer surface and at 40 cm from the outer surface are estimated for the RFQ and DTL with MARS code [7]. Figure 2 shows a the DTL model used in MARS where the bottom and top lines are the beam axis and the outer surface of the tank. In the figure, SS and SmCo stand for Stainless Steel and Samarium-Cobalt, constituent of a permanent magnet quadrupole used in the DTL. Dimensions of the drift tube in the figure is adjusted according to the proton beam energy. In the study, the beam loss is modeled as a proton beam incident on a point of the inner wall of the drift tube. The beam loss is often quoted as loss density in units of W/m. A detailed study showed that a point source gives the worst activation both on the outer surface and the 40 cm location compared when the same energy and power of protons are incident on either multiple spots or uniformly on a line [4]. Hence, to make a pessimistic estimate, a point source is assumed. Two cases when the

*ryoichi.miyamoto@esss.se

Figure 1: Schematic layout of the ESS linac.
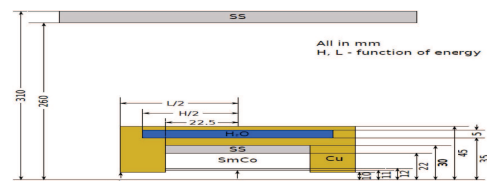
Figure 2: DTL model used in MARS. SS and SmCO stand for Stainless Steel and Samarium-Cobalt.
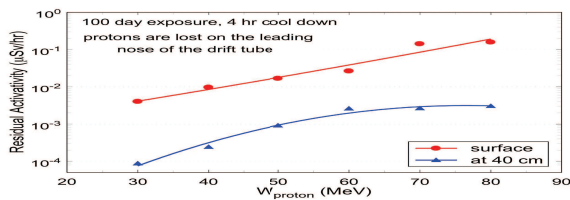
Figure 3: Residual dose rate on the outer surface and at the 40 cm location of the DTL tank due to 1 W proton loss.

source is at the center and the leading edge of the drift tube are compared and the activation is higher for the latter case. Hence, again to make a pessimistic estimate, only the latter case is considered. Figure 3 shows residual does rate on the outer surface and at the 40 cm location when exposed to losses for 100 days followed by four hours of a cool down time. The energy of the incident protons is varied from 30 MeV to 80 MeV, given the does rate due to proton below 30 MeV is too low and the DTL accelerates protons up to 79 MeV, whereas the power is kept at 1 W since the dose rate is proportional to the power of the incident protons and the result for a different power can be easily scaled from the for 1 W. The figure indicates that, even for 80 MeV protons, the dose rates at the 40 cm location is almost four orders of magnitude smaller than the CERN's criteria of 15 μSv/hr.

Figure 4 is from the same calculation as Fig. 3 but the result is converted to the power and current of the lost protons which produces the dose rate of 15 μSv/hr. Even for 80 MeV protons, about ~100 W of protons must be lost to produce 15 μSv/hr on the outer surface and more than 1000 W is necessary at the 40 cm location. A similar study is also conducted for RFQ and it is found that the proton energy of 3 MeV is too small to produce significant activations even on its outer surface [4]. These conclude that, from the point of view of activation of the components, losses in RFQ can be simply ignored and those in the DTL have a two orders of magnitude or even larger margin with respect to the often quoted 1 W/m. Similar studies are planned for the components in SCL.

TRACKING SIMULATION

To minimize the beam loss, it is ideal if patterns of beam losses could be predicted for given machine conditions by a tracking simulations. For the proton beam of 2.5 GeV and 5 MW, beam loss of 1 W corresponds to 2×10^{-7} of one
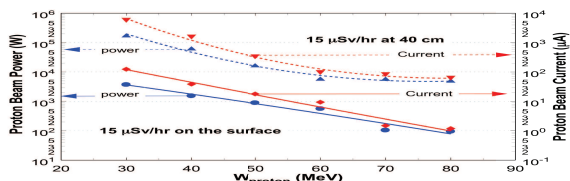
Figure 4: Power and current producing 15 μSv/hr does rate.

bunch, translating to 20 particles in a tracking simulation of as many as 100 million macro particles. Such a level of a simulation requires very accurate information of the particle distribution out of the ion source and electromagnetic fields of all the lattice elements including realistic estimates of alignment, static, and dynamics errors and also accurate modeling of relevant physics such as transport of particles through each element and space charge force. It is not yet clear to us that such a level of accuracy can be achieved but the plan is to make as realistic as possible predictions with available resource [8].

Now the lattice design being converging, studies of static lattice errors have been initiated using the TraceWin code [9], first for SCL only [2] given that the warm sections are not sensitive to beam losses as the often quoted 1 W/m as discussed in the previous section. Table 1 summarizes errors in the worst case tested thus far but no loss is observed after 1×10^5 macro particles are tracked in 1000 linacs with different random seeds. This proves the robustness of the present linac design but, to understand the beam loss pattern, further studies must be performed by applying errors worse than these and also including dynamics errors as well as errors in parameters of the incoming beam.

Table 1: List of Quadrupole and Cavity Errors in the Worst Case Tested thus far. The errors are distributed uniformly and the listed number is the maximum value.

Quadrupole	
Alignment in x and y [mm]	0.3
Rotation around z axis [mrad]	1
Gradient [%]	0.75
Cavity	
Alignment in x and y [mm]	3
Rotation around x and y axes [mrad]	3
Accelerating field strength [%]	1.5
Accelerating field phase [deg]	1.5

MEBT COLLIMATION

A pragmatic approach of reducing beam losses is to remove the beam halo in an early part of the linac. Based on the experience in the SNS linac [10], a few collimators are planned to be installed in the MEBT. Design of the MEBT has been revised since the beginning of 2012 and quality of the beam coming out the MEBT has been improved [11, 12]. Figure 5 shows the present design of the MEBT and three locations with tight apertures at proposed locations of collimators, with which the beam quality can be further improved.

Collimator Temperature Analysis

To estimate acceptable beam losses to a collimator in the MEBT, a simulation is performed with Fluka code [13] and
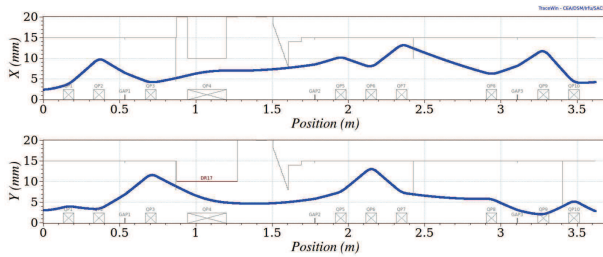
Figure 5: Layout and full beam (3σ) envelopes of the MEBT in the present design.

Figure 6: Halo particles in y plane at the end of the MEBT (colored) tracked back to the middle and entrance of the MEBT. Gray points represent particles in the core at the end of the MEBT.

ANSYS software [14]. The simulation assumes the collimator is made of graphite and placed at $3\sigma_x$ from the center of a two dimensional Gaussian beam and calculates the peak temperature within the collimator after exposed to one beam pulse. Beyond ~1500 C°, graphite may suffer from a mechanical damage so this simulation is to identify the smallest beam sizes acceptable to this collimator. A beam with halo in a real machine usually has a longer tail than a Gaussian beam and so the assumption of the Gaussian beam is pessimistic when estimating the temperature rise. There is no general criterion to distinguish the core and halo of a beam. The placement of the collimator at 3σ is chosen, as discussed in the following, because it is feasible from the point of view of the temperature limit of graphite and also the particle distribution at the end of the linac can be improved by a set of collimators placed at 3σ whereas it is barely affected by a set placed at 4σ. Table 2 summarizes the result of the simulation and indicates that this collimator should not be place at 3σ where RMS beam sizes in x and y are both as small as 1 [mm]. Removing particles beyond 3σ from the Gaussian beam with the same parameters as the beam in the MEBT corresponds to ~15 W absorbed by a collimator. In simulations of the following two sections, this 15 W is used as the maximum allowed loss in a collimator. The presented simulation and derived 15 W criterion are based on fairly simple assumptions and more detailed studies as well as an investigation of other materials than graphite are planned.

Table 2: Peak Temperature Inside a Graphite Collimator for Different Beam Sizes (a Collimator Placed at $3\sigma_x$)

σ_x [mm]	σ_y [mm]	Temperature [C°]
1	1	3017
1	2	1430
2	2	1178

Optimum Collimator Locations

A recent study [15] showed that a typical scheme using a set of collimators separated by a fix value of phase advance, such as two collimators separated by 90 degrees, may not be optimum for the MEBT since the space charge force is
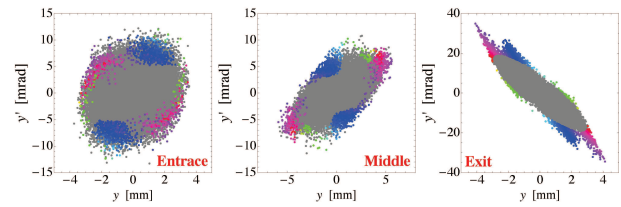
so strong that the phase advance of an each particle differs a lot depending on its phase space position at the entrance of the MEBT. On the other hand, because possible locations of collimators are limited due to mechanical constraints, a primitive method of finding an optimum set of collimator locations, such that first defining halo particles at the end of the MEBT and then observing their distribution at potential collimator locations, works reasonably well. Figure 6 shows particles beyond 3σ in y phase space at the end of the MEBT and also shows their distribution at the entrance and near the middle (at the chopper target with s=1.61 m). By comparing such distributions at mechanically possible locations, a set of locations in Fig. 5 is determined. The placement of each collimator with respect to the beam center is determined from the 15 W criterion of the previous section where the losses are calculated by tracking simulations. We note that some particles are showing chaotic behavior (namely two particles close to each other at the end of the MEBT may not be close to each other at the entrance of the MEBT) and so a risk to remove unnecessary particles together with the halo is higher for a collimator in an earlier part of the MEBT.

Improvement of Particle Distribution

The influence of the collimator set, determined in the previous section, on the beam is tested with TraceWin. Figure 7 compares the distributions in the transverse planes at the end of the MEBT in the cases with and without the col-
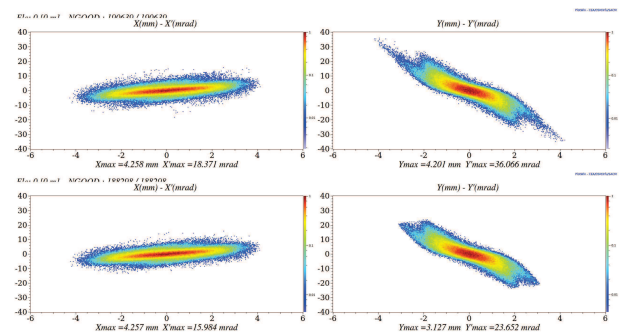
Figure 7: Distribution in x and y planes at the end of the MEBT with (top) and without (bottom) the collimators.
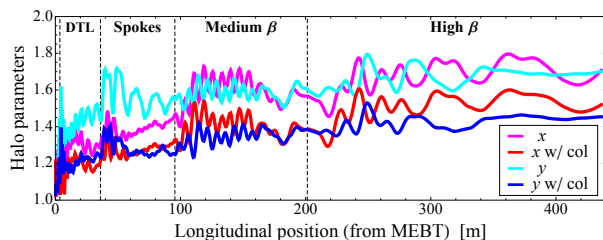
Figure 8: Halo evolution with and without the collimators.

limators. Reduction of the beam halo is visible, particularly for y plane, but the distribution is still not in an elliptical shape. If this is identified as an issue in future error studies of the downstream sections, the collimators must be placed closer to the beam, requiring a revision of the temperature analysis with more details.

Figure 8 shows evolution the halo parameters (see [16]) for definition of the halo parameters) throughout the linac in the cases with and without the presented set of collimators. The beam halo is well controlled in the present lattice but the case with the collimators is better, demonstrating that the collimation in the MEBT could improve the distribution at the end of the linac.

HEBT COLLIMATORS

The HEBT will include a collimation system to protect the proton beam window (PBW) and vital target, referred to as *a fixed collimator*. The HEBT contains aperture restrictions in vacuum chambers of dipoles and even more so in those of octupoles where large transverse beam size aspect ratios are intentionally sought. Hence, another system of collimators, referred to as *an adjustable collimator system*, is also considered to protect the accelerator components in the HEBT. A location immediately following the SCL, where mis-steered beams of anomalous energy is expected to occur during the commissioning, is a candidate to place the movable collimator. The collimator system would be built to withstand both slow and fast losses.

Optics in HEBT collimator sections

A non-linear beam expander system is designed to flatten the beam profiles at the PBW and main target station. Setting the utilized octupoles at strengths sufficient to modify the beam core, the halo is readily over-focused. The fixed collimator with fixed aperture is placed immediately upstream of the PBW and main target to intercept these tails before reaching sensitive components. The ongoing development of the beam profiles on the target surface drives the design of the fixed collimator. Variations of the expander optics have shown beam losses of the order of 5–25 kW for the nominal 5 MW beam. The adjustable collimators could complement and relieve the fix collimator.

The first 100 m section of the HEBT contains six periods of a doublet channel similar to the final part of the

SCL. Future power and or reliability upgrades can thus be introduced by installing cavities in the prepared slots. Until such an extension is performed, this section seems like the most appropriate area to place the adjustable collimators. They are expected to be employed mostly in the early years of operating the SCL where extensive halo should be expected. Eventually, one should learn to operate without relying on the adjustable collimators, thus enabling the SCL extension while removing the adjustable collimators.

Due to the single-pass nature of the HEBT, a proper halo reduction in each normalized phase space (NPS) requires repeating the collimation units after an appropriate phase advance $\phi_{11} = \pi/N_1$, where N_1 is the number of primary collimation units including two jaws for each transverse dimension. The upgrade section of the HEBT has a transverse phase advance of $\sim\pi/6$ per period, making either a □- ($N_1 = 2$) or ○-cut ($N_1 = 3$) in each NPS practical. In both cases, one or more smaller absorbers could be necessary to mask *e.g.* quadrupoles from intercepting particles with large scattering angles. For now, the minimum □-cut, single-stage collimator system is assumed.

Mechanical Considerations

The four jaws per collimation unit are typically introduced by two subunits each setting a cut in either the same directions (opposing jaws) or mixed directions (L-shaped jaws). The latter has been used *e.g.* in the FNAL MI8 [17] and J-PARC 3–50BT [18] transfer lines. In both cases, vacuum feedthroughs and insertions have been limited to attain high reliability and avoid the need for hands-on maintenance. Each L-jaw will be placed in a rectangular vacuum pipe (the collimator duct) which is fixed in a movable external radiation shield. Removal of the external shield should never be necessary, and the end-flanges of each duct would be manipulated remotely using specialized tools. Thermocouples will monitor the temperature rise, while ionization chambers will be placed to monitor the beam loss versus jaw position. The jaws could possibly also be electrically isolated to measure the deposited current.

Motors and electronics will be placed strategically behind the radiation shield to reduce the exposure to radiation. Lubrication of these movable parts should also consider rad-hard oils.

Studies of Collimation Efficiency

To study collimation efficiency and overall feasibility, a geometry and the appropriate quadrupole fields are implemented in MARS [7]. For simplicity, only a horizontal (1D) collimator system is assumed, however the use of L-shaped jaws is anticipated. In the 1D case, a collimator system thus consists of two consecutive subsystems including a left and right jaw, respectively. In Fig. 9, a cross section of a collimator subsystem is shown. Rectangular collimator jaws consisting of $20 \times 100 \times L_{jaw}$ mm^3 ($H \times W \times L_{jaw}$) of stainless steel (SS316) are modeled. These are placed in a rectangular collimator duct of $100 \times 100 \times 1300$ mm^3,
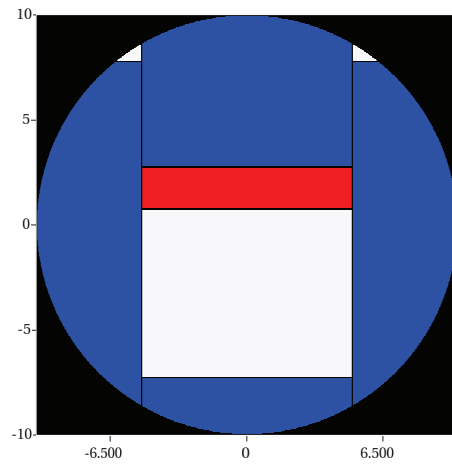
Figure 9: Cross section of a 1D collimator subsystem: the jaw is red and the shielding is blue. The entire unit is displaced horizontally to impose a cut ($x < 8$ mm).

Figure 10: Horizontal phase space density immediately following the $L_{jaw} = 800$ mm SS316 collimator.

essentially inscribing the circular HEBT vacuum pipe of $\varnothing 100$ mm inner aperture. The SS316 collimator duct volume extends several cm transversely to also represent parts of the external radiation shield. Jaw tapering will later be included to maximize the impact parameter. As input beam for MARS, particles in the 4D transverse NPS are sampled from distribution functions. The vertical NPS is modeled by a 2D Gaussian distribution. For the RMS normalized emittance of the core distributions, we assume $0.25\ \pi$ mm mrad in both transverse planes. In the horizontal NPS only an exponential halo distribution band is generated in the region $3.3 \leq n_1 \leq 10$, where n_1 is the particle radius in the NPS in units of RMS. Collimation is considered to the level of $n_1 \geq 3.4$ beyond which a fractional halo of $f_{halo} = 3.09 \times 10^{-3}$ is assumed to be, corresponding to 15.4 kW of beam power in the band being probed by collimators. With the current HEBT optics, this corresponds to a minimum collimator half-gap of $\sim$7.3 mm. Due to the overall collimator system's non-circular cut in the horizontal NPS, $\sim$12 kW will be intercepted by the four jaws in the horizontal plane, leaving about 3 kW per jaw, which is considered the limiting case.

In Fig. 10, the horizontal phase space after a single subunit is seen. With $L_{jaw} = 800$ mm of SS316 jaws, the outscattered particles ($x, x' < 0$) dominate, although traces of particles traversing the jaw ($x, x' > 0$) can be seen. Under these circumstances, $\sim$6% of the protons touching the jaws are transmitted, albeit at reduced energy. The populated emittances clearly exceed the HEBT's admittance, also shown in Fig. 10, hence masks and absorbers will have to be strategically placed to handle this.

Introducing single-stage collimation in the S1 comes at a cost, as it inevitably introduces secondary losses downstream, possibly violating the principle of $\lesssim 1$ W/m loss. Justification and further design of the systems will greatly benefit from input on typical collimator operational experience at existing high-power facilities and studies of fault
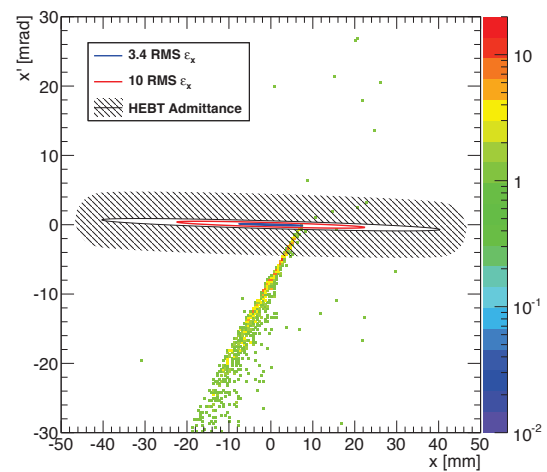
scenarios. A SCL beam with a large closed orbit deviation should be studied; both in terms of implications to the collimators but also to the beam delivered to the target.

CONCLUSIONS

One of the biggest challenges in design and operation of the 5 MW ESS proton linac is to minimize beam losses and this requires efforts in various aspects of accelerator science and engineering. This paper presented the present status of on-going studies in the beam loss limit, tracking simulation, and the MEBT and HEBT collimation schemes.

REFERENCES

[1] ESS Report No. ESS-2012-001, 2012.

[2] M. Eshraqi *et al.*, TUO3B02, this proceedings.

[3] L. Tchelidze, ESS AD Technical Note No. ESS/AD/0031, 2012.

[4] J. Stovall and L. Tchelidze, ESS AD Technical Note No. ESS/AD/0039, 2012.

[5] http://www.stralsakerhetsmyndigheten.se/
Global/Publikationer/Forfattning/Engelska/
SSMFS-2008-51E.pdf

[6] P. Jacobsson, ESS-0000004, 2011.

[7] N. V. Mokhov, Fermilab-FN-628, 1995; N. V. Mokhov and S. I. Striganov, HSS'06, p. 50, 2006.

[8] H. Danared *et al.*, ICAP'12, to be published.

[9] R. Duperrier *et al.*, ICCS'02, LNCS 2331, p. 411, 2002.

[10] D. Jeon *et al.*, PRST-AB **5**, 094201 (2002).

[11] M. Eshraqi *et al.*, IPAC'12, THPPP085, 2012.

[12] I. Bustinduy *et al.*, MOP235, this proceedings.

[13] G. Battistoni *et al.*, Hadronic Shower Simulation Workshop 2006, p. 31 (2007); A. Fasso *et al.*, CERN-2005-10, INFN/TC_05/11, SLAC-R-77, 2005.

[14] "Ansys Simulation Code".

[15] R. Miyamoto *et al.*, IPAC'12, MOPPD076, p. 541. 2012.

[16] C. K. Allen and T. P. Wangler, PRST-AB **5**, 124202 (2002).

[17] V. Sidorov *et al.*, Fermilab-beams-doc-2287, 2006.

[18] M. J. Shirakata *et al.*, EPAC'06, TUPCH060, 2006.